ELSEVIER

Applied Surface Science 174 (2001) 225–231

applied surface science

www.elsevier.nl/locate/apsusc

Surface processes on Si(1 1 1)7×7 and SiO_2 mediated by low-energy ion irradiation in CF_4

Zhenhua He, K.T. Leung*

Department of Chemistry, University of Waterloo, Waterloo, Ontario, Canada N2L 3G1

Received 17 November 2000; accepted 28 January 2001

Abstract

The surface reactions of the 7×7 and oxidized surfaces of Si(1 1 1) mediated by ion irradiation in CF_4 at 50 eV impact energy have been investigated by using electron energy loss spectroscopy (EELS), thermal desorption spectrometry (TDS) and low energy electron diffraction (LEED). The reaction layer for the fluorocarbon-ion-irradiated Si(1 1 1)7×7 sample is characterized by the presence of Si–C stretching, Si–F_x ($x = 1-3$) stretching and bending modes in the EELS spectra. The lack of any observable C–F stretching feature in the EELS spectra further indicates the absence of any appreciable amount of as-formed CF_x ($x = 1-3$) surface species. The TDS results also show that SiF_4 is the major desorption product and CF_x desorption products are not observed. These results therefore suggest that SiC and SiF_x ($x = 1-3$) make up the reaction layer when Si(1 1 1)7×7 is ion-irradiated with a high exposure of CF_4 at low impact energy. When oxidized Si(1 1 1) is irradiated by the same dose of fluorocarbon ions, evidence for deposition of more SiF_x but less SiC species (relative to the 7×7 surface) is found, which indicates that the surface O may combine with surface C to form gaseous CO or CO_2, leaving behind more F to react or bind with the Si substrate atoms. The corresponding TDS data suggests that the OCF radical may be one of the minor desorption products.

Keywords: Electron energy loss spectroscopy; Chemisorption; Ion irradiation

1. Introduction

Chemical vapor deposition and chemical etching involving halocarbon plasmas on silicon substrate have been used extensively in the microelectronics industry [1]. Fluorocarbon films can be deposited under appropriate plasma conditions and the formation of these films can in turn affect directional etching [2–4]. The energy of the ions plays an important role in plasma chemistry and plasma-surface interactions [5]. By modifying this and other plasma conditions, the plasma equilibrium can be shifted between the deposition and etching regimes. In spite of the extensive studies on the effects of ion bombardment on silicon [6–10], the interactions of fluorocarbon ions with Si remain poorly understood, especially for bombardment energy below 100 eV. Of considerable interest is the determination of the appropriate kinematic conditions (flux, kinetic energy, etc.) of the ions and radicals in the plasma for deposition of polymer films involving gas-phase polymerization [2]. Coburn and Winters have shown that there is a balance between etching and polymerization that depends on the F to C ratio of the precursor of the plasma [11]. Some attempts to understand the mechanisms of plasma-mediated processes have been made under simplified conditions using XeF_2 and F_2 [5,6]. Bello

* Corresponding author. Tel.: +1-519-746-0435.
E-mail address: tong@uwaterloo.ca (K.T. Leung).

0169-4332/01/$ – see front matter
PII: S0169-4332(01)00175-1

et al. employed mass-separated low-energy molecular ion beams to study specific ion mediated surface processes [8,9], while Oehrlein investigated the effects of ion bombardment on the reaction layer under realistic plasma conditions [10]. Since modern manufacturing of the next-generation devices involves such key steps as selective etching of SiO_2 over Si with a high-aspect ratio, a better understanding of the complex plasma chemistry and its effects on the substrate would be of great interest.

In the case of fluorocarbon plasma etching of Si or SiO_2, the formation of a thin fluorocarbon or fluorinated silicon oxide (SiOF) reaction layer has been observed [12]. Along with fluoropolymer, fluorinated amorphous carbon and fluorocarbonated SiO_2 films, SiOF films have attracted a lot of recent attention because of their low dielectric constant, which makes them viable candidates as a new type of inter-metal dielectric materials for microelectronic applications. In particular, the incorporation of fluorine in these materials changes the Si–O network to a less polarizable geometry, resulting in a reduction of the dielectric constant. The formation of these fluorocarbonated SiO_2 films is usually achieved by plasma enhanced chemical vapor deposition [12]. A better understanding of the fluorocarbon-surface interaction will provide new insight into the early stage of formation and the subsequent reactions of this type of films.

Although many well established surface diagnostic techniques including X-ray photoelectron spectroscopy, Auger electron spectroscopy (AES), and Fourier transform infrared spectroscopy have been used to investigate the surface processes induced by ion irradiation of halocarbons [8,9,13–16], there is no study involving the more surface-sensitive electron energy loss spectroscopy (EELS). In the present work, we study the surface processes on clean and oxidized surfaces of Si(1 1 1)7×7 as a result of ion irradiation in CF_4 at 50 eV impact energy by using vibrational EELS, thermal desorption spectrometry (TDS) and low energy electron diffraction (LEED). Possible surface species and reaction processes are identified.

2. Experimental

Details of the experimental apparatus used in the present work have been given elsewhere [17]. All the experiments were performed in a home-built ultra-high vacuum chamber with a base pressure better than 1×10^{-10} Torr, achieved by a combination of 170 l/s turbo molecular pump, a 230 l/s ion pump, and a 2000 l/s titanium sublimation pump. The chamber was equipped with an ion (-sputtering) gun, a 4-grid retarding-field optics for both reverse-view LEED and Auger electron spectroscopy (AES), a 1–300 amu quadrupole mass spectrometer (QMS) for TDS studies, and a home-built multi-technique EELS for both electronic and vibrational EELS measurements. The QMS was housed in a separate chamber that was differentially pumped by a 60 l/s ion pump. The EELS spectrometer used for the present work has also been described in detail in [18]. In the present vibrational EELS study involving Si surfaces roughened by low-energy ion irradiation, a routine energy resolution of 15–22 meV (120–180 cm^{-1}) full-width at half-maximum (FWHM) can be achieved with a typical count rate of 100,000 counts per second for the elastic peak, at a typical impact energy of 5 eV. For electronic EELS measurements involving a higher impact energy, the energy resolution becomes 30 meV FWHM. Our spectrometer therefore offers adequate performance for most of our applications on the Si substrate, covering both vibrational studies at reasonably high resolution and electronic structural investigations over an extended energy loss range [17,18].

The Si(1 1 1) sample (p-type boron doped, 50 Ω cm, 8 mm × 6 mm × 0.5 mm thick) with a stated purity of 99.999% was purchased from Virginia Semiconductor Inc. The sample was mechanically fastened to a Ta sample plate with 0.25 mm-diameter Ta wires. Heating of the Si sample was achieved by electron bombardment from a heated tungsten filament at the backside of the sample. The Si(1 1 1) sample was cleaned by using a standard procedure involving repeated cycles of Ar^+ sputtering and annealing to 1200 K until a sharp 7×7 LEED pattern was observed. The cleanliness of the sample was further verified in situ by the lack of any detectable vibrational EELS feature attributable to unwanted contaminants, particularly the Si–C peak at 800–820 cm^{-1}. The gaseous samples, carbon tetrafluoride and oxygen (all at 99.99% purity), were purchased from Matheson and used without further purification.

Ion irradiation (without mass selection) was performed by operating the ion gun with the chamber

back-filled with the gas of interest to a working pressure of 1×10^{-6} Torr. The sample was positioned 5 cm from the front face of the ion gun during the ion irradiation experiments. The impact energy of the ion beam could be controlled by adjusting a floating voltage applied on the sample with respect to a pre-selected beam energy of the ion gun. The ion dose can be estimated by the product of the ion flux (estimated to be $\sim$2 nA/mm^2) and the exposure time (obtained from the exposure in units of Langmuir ($1\,\mathrm{L} = 1 \times 10^{-6}$ Torr s) and the working pressure employed (1×10^{-6} Torr)). In the present experimental setup, the reactant gases were ionized by electrons with 180 eV kinetic energy inside the ion gun and only positive ions from the ion gun could reach the sample without mass selection. The concentration of each ion can be estimated from the cracking pattern of the corresponding molecule reported in the literature [19]. In the case of CF_4, CF_3^+ is the majority or base ion (estimated to be 78%), with other smaller ions such as CF_2^+ (10%) and CF^+ (3%) present at lower concentrations [32]. When the ions collide with the surface, they may become neutralized and undergo further dissociation into other smaller fragments including C and F atoms. The resulting fragments and radicals may subsequently react with the substrate atoms and/or other pre-deposited surface species.

3. Results and discussion

Fig. 1 shows the typical vibrational EELS spectra of Si(1 1 1)7×7 sputtered in CF_4 at 50 eV impact energy as a function of exposure at room temperature (RT). Only one EELS feature at 780 cm^{-1} is observed at 1 kL (1 kL = 1000 L) and it appears to blue-shift gradually with increasing ion dose to 885 cm^{-1} at 10 kL. A weak feature near 340 cm^{-1} emerges as a shoulder at 2.5 kL and becomes a well-defined peak at higher exposure (10 kL). According to the published infrared spectroscopic data for inorganic materials [20–24], the Si–F stretching mode usually occurs at 825–850 cm^{-1}, while the Si–F_x ($x = 2$ or 3) symmetric and asymmetric stretching modes appear at 827–870 and 920–1015 cm^{-1}, respectively. Given also that the Si–C stretching mode is commonly observed at 800–820 cm^{-1} [25,26], the vibrational peak at the higher energy loss (780–885 cm^{-1}) can

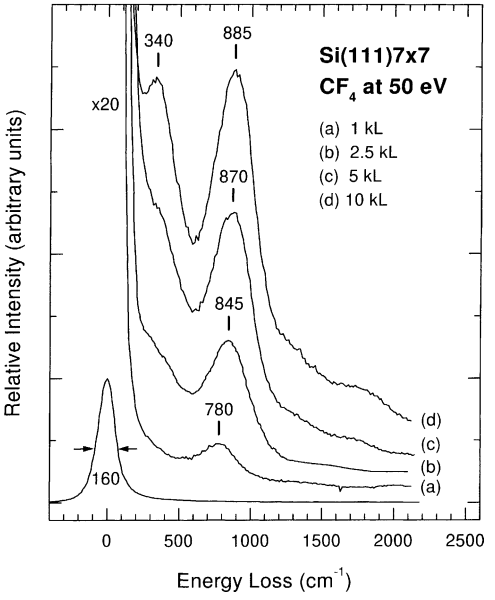

Fig. 1. Vibrational electron energy loss spectra for Si(1 1 1)7×7 ion-irradiated at 50 eV impact energy in: (a) 1 kL; (b) 2.5 kL; (c) 5 kL; (d) 10 kL of CF_4.

be attributed to a combination of Si–C and Si–F_x ($x = 1-3$) stretching modes. The feature at 340 cm^{-1} can be assigned as the Si–F_x bending mode [20–24]. The EELS data clearly shows that SiC and SiF_x are the predominant products on Si(1 1 1)7×7 as a result of ion irradiation with increasing CF_4 exposure. In the case of SiF_x, the lack of a bending mode (the low energy loss feature) suggests that only SiF is formed at low exposure (1 kL), while the emergence of the bending mode at 340 cm^{-1} provides evidence for the formation of SiF_2 and SiF_3 surface species at higher exposure. The blue shift of the higher energy loss feature (from 780 to 885 cm^{-1}) with increasing exposure is also consistent with increasing contribution from the Si–F_x symmetric and asymmetric stretching modes of SiF_2 and SiF_3 that occur at higher energy loss. Since no discernible feature at $\sim$1024 cm^{-1}, commonly attributable to C–F stretching modes [27], is observed, there is no evidence for the presence of CF_x species on the surface. This result is in accord with the earlier work reported by Winters and Coburn [5], which showed that most of the CF_x^+ ions completely dissociate into C and F atoms upon impact with the Si surface. Chemisorption of the resulting C and F atoms on the Si substrate leads to

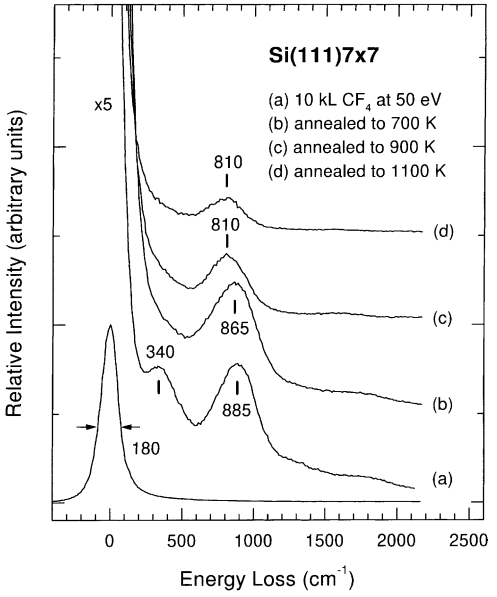

Fig. 2. Vibrational electron energy loss spectra for Si(1 1 1)7×7 ion-irradiated at 50 eV impact energy in: (a) 10 kL of CF_4 and followed by annealing; (b) 700 K; (c) 900 K; (d) 1100 K.

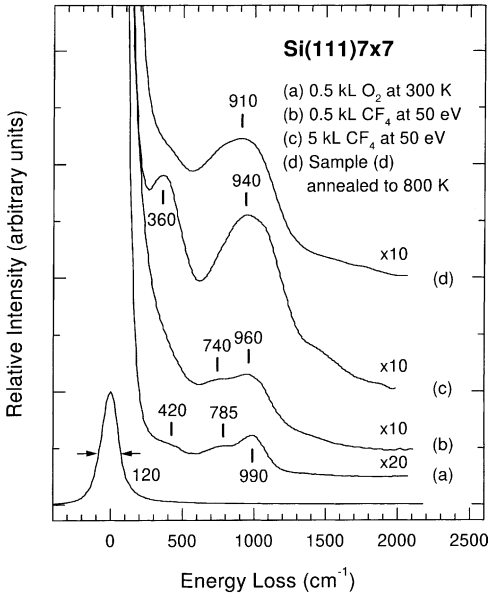

Fig. 3. Vibrational electron energy loss spectra for Si(1 1 1)7×7 (a) after oxidation by exposure of 500 L of O_2 at room temperature, and subsequently ion-irradiated at 50 eV impact energy in (b) 0.5 kL and (c) 5 kL of CF_4, followed by (d) annealing to 800 K.

the various SiC and SiF_x species with the characteristic energy loss features mentioned above. The nature of this type of "disordered" SiC surface species has been examined in more detail by other techniques (including electronic EELS and AES) in our earlier work [30] and is believed to involve Si–C bonds not necessarily fully terminated.

Fig. 2 depicts the effect of annealing on the fluorocarbon-ion-irradiated sample shown in Fig. 1d. Annealing the sample (Fig. 2a) to 700 K appears to remove the Si–F_x bending features at 340 cm^{-1} (Fig. 2b), which indicates desorption of the SiF_2 and SiF_3 species from the surface. Further successive annealing to higher temperature not only reduces the intensity of the broad peak at 885 cm^{-1} but also causes a red shift back to a lower frequency of 810 cm^{-1} (characteristic of the Si–C stretching mode), which is consistent with the continual desorption of SiF from the surface, leaving behind SiC above 900 K (Fig. 2c).

The changes in the LEED pattern of the Si sample have also been monitored during the annealing experiment. After ion irradiation with 1–5 kL of CF_4 at 50 eV impact energy, the 7×7 LEED pattern became a 1×1 pattern, which reverted back to a weak and diffuse 7×7 pattern when the sample was annealed to 900 K. Ion irradiation with a heavier dose (10 kL) of CF_4 at 50 eV resulted in no discernible LEED pattern, which became a weak 1×1 and then a 7×7 pattern upon annealing to 900 and 1100 K, respectively.

Fig. 3 shows the effect of ion irradiation in CF_4 at 50 eV impact energy on an oxidized Si surface. The oxidized surface was obtained by exposing 500 L of O_2 at RT and is characterized by three energy loss features at 420, 785 and 990 cm^{-1}, corresponding to, respectively, rocking, symmetric and asymmetric stretching modes of the Si–O–Si radical [28,29]. Unlike the vitreous SiO_2 in silica with a Si–Si separation of 3.05 Å, the Si−Si separation of the oxide layer formed at RT is essentially the same as that in crystalline silicon (2.35 Å). The SiO_2 layer formed at RT therefore has a more "compressed" structure with a smaller angle between the two Si–O bonds than the vitreous SiO_2. The latter can be obtained by annealing the sample after and/or during oxidization to 700 K or by ion-bombarding the sample in O_2 at RT [30]. The vibrational features for vitreous SiO_2 are found to be blue-shifted by approximately 80–100 cm^{-1} from the corresponding features of "normal" SiO_2 formed at

RT [30]. After ion irradiation of the oxidized surface with increasing exposure of CF_4 (0.5 kL in Fig. 3b and 5 kL in Fig. 3c), the energy loss feature at 420 cm^{-1} becomes a well-defined peak at 360 cm^{-1} attributable to Si–F_x bending modes (Fig. 3c), while the higher energy loss features begin to merge into a single broad band at 940 cm^{-1}, which can be attributed to a combination of the O–Si–O stretching modes and the Si–C and Si–F_x stretching features observed earlier (Fig. 1). Annealing the resulting sample to 800 K completely removes the feature at 360 cm^{-1} and causes the broad higher energy loss feature to undergo an apparent red shift to 910 cm^{-1}, which can be assigned as before to a combination of Si–C and Si–F_x stretching modes (Fig. 3d). Despite the limited energy resolution inherent in the present work involving roughened surfaces, we can clearly differentiate the Si–F_x bending modes at 360 cm^{-1} (Fig. 3c) from the O–Si–O rocking mode at 420 cm^{-1} (Fig. 3a), especially given the large difference in their intensities. Annealing to 800 K therefore appears to consolidate the formation of an overlayer composed predominantly of SiC and SiF_x species on the oxidized surface.

Following Ibach et al. [28], we prepared a vitreous SiO_2 layer (of approximately 5 Å thick) by dosing 10 kL O_2 with the sample Si(1 1 1)7×7 held at 700 K, which exhibits a weak 1×1 LEED. A relatively thick oxidized layer was prepared in order to study the reaction of CF_x^+ ions with surface oxygen in excess. Fig. 4 compares the EELS spectrum of Si(1 1 1)7×7 with that of the oxidized Si surface, each after ion irradiation in 10 kL of CF_4 at 50 eV impact energy at RT. Ion irradiation in CF_4 does not appear to produce any marked difference between the EELS spectra for the vitreous SiO_2 layer (Fig. 4b) and the oxidized layer produced at RT (Fig. 3c). We have seen in our earlier work that sputtering in O_2 can also generate vitreous SiO_2 on Si(1 1 1)7×7 at RT [30]. We believe that sputtering in CF_4 in the presence of surface oxide can also induce the formation of vitreous SiO_2 at RT due to the breakage of the Si–Si back bonds caused by the sputtering process. Evidently, the Si–F_x bending feature at 340–360 cm^{-1} becomes more intense on the oxidized Si surface (Fig. 4b) relative to that of the 7×7 surface (Fig. 4a), which clearly shows that more SiF_x ($x = 1-3$) species are produced on the oxidized Si surface. The presence of oxygen on the oxidized surface facilitates the removal of carbon on the surface

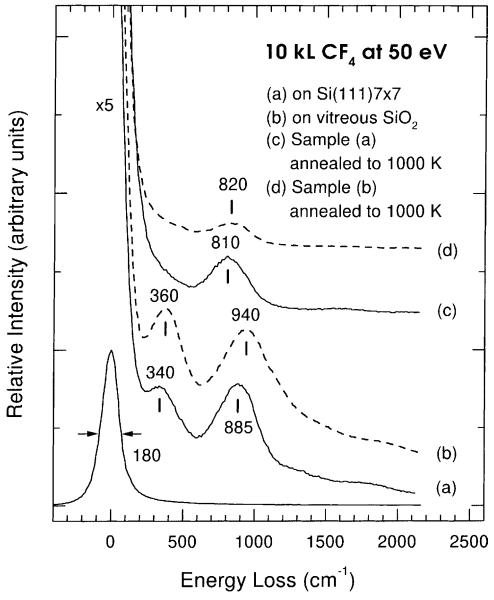

Fig. 4. Vibrational electron energy loss spectra for (a) Si(1 1 1)7×7 and (b) a vitreous SiO_2 surface, both after ion irradiation in 10 kL of CF_4 at 50 eV impact energy, and for annealing both (c) sample (a) and (d) sample (b) to 1000 K. The vitreous SiO_2 surface was obtained by exposing Si(1 1 1)7×7 to 10 kL of O_2 at 700 K.

and hence opens up additional binding sites for surface F atoms. Furthermore, there is a blue shift of 55 cm^{-1} in the higher energy loss feature for the oxidized surface (940 cm^{-1}) relative to the 7×7 surface (885 cm^{-1}), which could be attributed to the coupling of Si–O_x ($x = 1, 2$) vibrations to the existing Si–C and Si–F_x stretching modes [31]. Annealing the samples to 1000 K removes the low energy loss feature completely from both spectra, which is consistent with the earlier observation that SiF_2 and SiF_3 surface species desorb above 700 K (Fig. 2). As shown also in Fig. 2, annealing above 900 K would desorb SiF species from the surface, which is consistent with the red shift of the higher energy loss feature back to 810–820 cm^{-1} (characteristic of the Si–C stretching mode) upon annealing the corresponding samples to 1000 K (Fig. 4). A similar red shift in the higher energy loss feature with increasing annealing temperature is also observed, when comparing Fig. 3d (800 K) with Fig. 4d (1000 K). As shown in Fig. 4d, the weaker Si–C feature for the oxidized sample suggests that the presence of O on the surface may facilitate recombi-

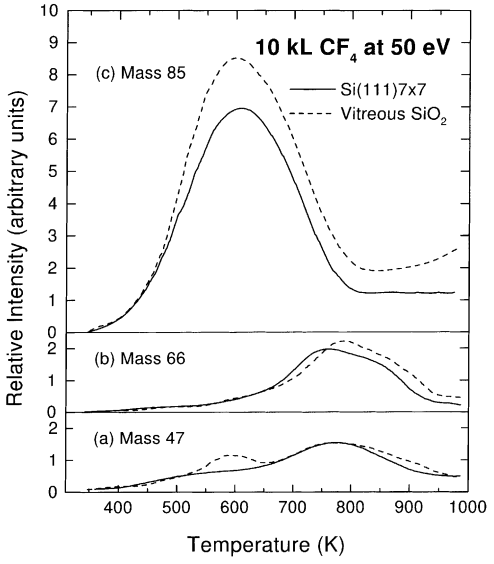

Fig. 5. Temperature programmed desorption profiles of (a) mass 47 (SiF^+ or OCF^+), (b) mass 66 ($SiF_2{}^+$), and (c) mass 85 ($SiF_3{}^+$) for Si(1 1 1)7×7 (solid lines) and a vitreous SiO_2 surface (dashed lines). The vitreous SiO_2 surface was obtained by exposing Si(1 1 1)7×7 to 10 kL of O_2 at 700 K.

native reactions with surface C to form gaseous CO and/or CO_2 and thus enhance the removal of surface carbon (reducing the corresponding Si–C peak).

Fig. 5 shows the corresponding TDS profiles of mass 85 ($SiF_3{}^+$), mass 66 ($SiF_2{}^+$), and mass 47 (SiF^+) for the Si(1 1 1)7×7 and vitreous SiO_2 surfaces after ion irradiation in 10 kL of CF_4 at 50 eV impact energy (corresponding to samples in Fig. 4a and b, respectively). Since $SiF_3{}^+$ corresponds to the predominant (∼90%) ion (base mass) in the gas-phase cracking pattern of SiF_4 [32], the strong desorption intensity found for mass 85 indicates that SiF_4 is the major desorption product. Similarly, $SiF_2{}^+$ and SiF^+ are found in comparable amounts from electron impact ionization of gaseous SiF_2 [5,33]. The TDS profile of $SiF_2{}^+$ (mass 66) is seen to be essentially identical to that of SiF^+ (mass 47), with a prominent desorption peak at ∼780 K, indicating that both ions originate from the same parent species, most likely SiF_2. On the other hand, the TDS profile for $SiF_3{}^+$ (mass 85) clearly has a different desorption maximum (600 K) than those for $SiF_2{}^+$ (mass 66) and SiF^+ (mass 47), which is consistent with the hypothesis that the latter two ions come from a different desorption product (SiF_2). Our TDS results are found to be similar to the results for gas-phase reaction products (SiF, SiF_2 and SiF_4 species) generated by other means, as reported by Winters and Coburn [5] and Engstrom et al. [34]. Although the TDS profiles for both samples are very similar, the TDS profile of mass 47 for the oxidized surface exhibits an additional desorption peak at 580 K. Since the base mass for OCF_2 corresponds to OCF^+ [35], which has the same mass 47 as SiF^+, the new TDS feature near 580 K could be due to OCF^+. However, given that there is no corresponding desorption feature at 580 K for mass 66, corresponding to the parent mass of $OCF_2{}^+$, the formation of OCF radical (instead of OCF_2) is therefore more likely. This result suggests that unlike the 7×7 surface, the presence of oxygen on the oxidized Si surface after ion irradiation in CF_4 makes possible recombinative desorption of surface O, (Si–)C, and (Si–)F, making OCF a plausible desorption product. Finally, we also monitored fluorocarbon fragments, including mass 69 ($CF_3{}^+$), mass 50 ($CF_2{}^+$) and mass 31 (CF^+) during the TDS experiments. The lack of any desorption feature for these masses confirms that no substantial CF_x species is formed on the Si(1 1 1)7×7 or vitreous SiO_2 surface as a result of ion irradiation in CF_4.

4. Summary

In the present work, we examine the surface processes on Si(1 1 1)7×7 and oxidized Si surfaces induced by ion irradiation in CF_4 at 50 eV impact energy. Our vibrational EELS data shows that SiC and SiF_x ($x = 1-3$) are produced on both 7×7 and oxidized surfaces as a result of low-energy ion irradiation in CF_4 at high exposure, while no evidence for the presence of CF_x species on these samples is found. Along with our TDS experiments, these EELS spectra further suggest that there is more SiF_x but less SiC formed on the oxidized Si surface than Si(1 1 1)7×7 by ion irradiation with the same dose of $CF_x{}^+$ ions. The surface C species may combine with surface O to form gaseous CO and/or CO_2, thus leaving a relatively higher F moiety to bind with the substrate Si atoms. The TDS results also suggest that OCF may be one of the desorption products for oxidized surfaces ion-irradiated in CF_4. Other studies conducted in our group show that the surface processes mediated by

ion irradiation in CF_4 at low impact energy (50 eV) are qualitatively similar to those at high impact energy (500 eV). This work illustrates some of the intricate ion surface chemistry during the early stage of plasma processing for common semiconductor materials.

Acknowledgements

This work was supported by the Natural Sciences and Engineering Research Council of Canada.

References

[1] G.S. Oehrlein, Surf. Sci. 386 (1997) 222.
[2] C.B. Labelle, K.K. Gleason, J. Vac. Sci. Technol. A 17 (1999) 445.
[3] R. d'Agostino, P. Capezzuto, G. Bruno, F. Cramarossa, Pure and Appl. Chem. 57 (1985) 1287.
[4] T. Shirafuji, W.W. Stoffels, H. Moriguchi, K. Tachibana, J. Vac. Sci. Technol. A 15 (1997) 209, and references therein.
[5] H.F. Winters, J.W. Coburn, Surf. Sci. Rep. 14 (1992) 161.
[6] J.W. Coburn, J. Vac. Sci. Technol. A 12 (1994) 1417.
[7] Y. Horrike, M. Shibagaki, K. Kadono, Jpn. J. Appl. Phys. 18 (1979) 2309.
[8] I. Bello, W.H. Chang, W.M. Lau, J. Vac. Sci. Technol. A12 (1994) 1425.
[9] W.H. Chang, I. Bello, W.M. Lau, J. Vac. Sci. Technol. A11 (1993) 1221.
[10] G.S. Oehrlein, J. Vac. Sci. Technol. A11 (1993) 34.
[11] J.W. Coburn, H.F. Winters, J. Vac. Sci. Technol. 16 (1979) 391.
[12] K.S. Oh, M.S. Kang, K.M. Lee, D.S. Kim, C.K. Choi, S.M. Yun, H.Y. Chang, K.H. Kim, Thin Solid Films 345 (1999) 45.
[13] K. Miyake, S. Tachi, K. Yagi, T. Tokuyama, J. Appl. Phys. 53 (1982) 3214.
[14] D.J. Thomson, C.R. Helms, Appl. Phys. Lett. 46 (1985) 1103.
[15] G.S. Oehrlein, J.G. Clabes, P. Spirito, J. Electrochem. Soc. 133 (1986) 1002.
[16] S.W. Robey, G.S. Oehrlein, Surf. Sci. 210 (1989) 429.
[17] D.Q. Hu, Ph.D. Thesis, University of Waterloo, Waterloo, 1993.
[18] H. Yu, D.Q. Hu, K.T. Leung, J. Vac. Sci. Technol. A 15 (1997) 2653.
[19] Eight Peak Index of Mass Spectra, Mass Spectrometry Data Center, Vol. 1, Aldermaston, 1974.
[20] K. Nakamoto, Infrared and Raman Spectra of Inorganic and Coordination Compounds, Wiley, New York, 1986, p. 132.
[21] L. Ley, H.R. Shanks, C.J. Fang, K.J. Gruntz, M. Cardona, J. Phys. Soc. Jpn., Suppl. A 49 (1980) 1241.
[22] T. Shimada, Y. Katayama, S. Horigome, Jpn. J. Appl. Phys. 19 (1980) L265.
[23] T. Shimada, Y. Katayama, J. Phys. Soc. Jpn., Suppl. A 49 (1980) 1245.
[24] K. Yamamoto, M. Tsuji, K. Washio, H. Kasahara, K. Abe, J. Phys. Soc. Jpn. 52 (1983) 925.
[25] J. Yoshinobu, H. Tsuda, M. Onchi, M. Nishijma, J. Chem. Phys. 87 (1987) 7332.
[26] J. Schmidt, C. Stuhlmann, H. Ibach, Surf. Sci. 302 (1994) 10.
[27] K. Nagai, C. Yamada, Y. Endo, E. Hirota, J. Mol. Spectrosc. 90 (1981) 249.
[28] H. Ibach, H.D. Bruchmann, H. Wagner, Appl. Phys. A 29 (1982) 113.
[29] G. Comtet, L. Hellner, G. Dujardin, M.J. Ramage, Surf. Sci. 353/354 (1996) 315.
[30] H. Yu, K.T. Leung, Surf. Sci. 432 (1999) 245.
[31] S.M. Han, E.S. Aydil, J. Vac. Sci. Technol. A 15 (1997) 2893.
[32] P.W. Harland, S. Cradock, J.C. Thyne, Int. J. Mass Spectrom. Ion. Phys. 10 (1972/73) 169.
[33] R.J. Shul, T.R. Hayes, R.C. Weitzel, F.R. Baicchi, R.S. Freund, J. Chem. Phys. 89 (1988) 4042.
[34] J.R. Engstrom, M.M. Nelson, T. Engel, Surf. Sci. 215 (1989) 437.
[35] NIST/EPA/NIH Mass Spectral Library, NIST'98 with Windows, Version 1.7 Software, 1996.